RAPID COMMUNICATIONS

PHYSICAL REVIEW B VOLUME 40, NUMBER 5 15 AUGUST 1989-I

Helium scattering studies of the dynamics of a xenon-monolayer-covered graphite single-crystal surface

J. P. Toennies and R. Vollmer
Sonderforschungsbereich 126 and Max-Planck-Institut für Strömungsforschung, Bunsenstrasse 10, D-3400 Göttingen, Germany
(Received 7 September 1988; revised manuscript received 8 March 1989)

The dispersion curves of the surface modes of a monolayer of xenon adsorbed on a single crystal of graphite have been measured by helium-atom scattering. A strong hybridization-induced splitting is observed between the localized adsorbate mode and the substrate Rayleigh mode, indicating a stronger adsorbate-substrate interaction than that for the case of rare gases on metals.

I. INTRODUCTION

One of the most intriguing problems in surface science is that of two-dimensional phase transitions involving a monolayer adsorbate on a single-crystal substrate.[1] The microscopic and macroscopic dynamical behavior of the system is largely determined by the competition between the lateral interaction of the adsorbed particles and the interaction of the adsorbate with the substrate. The different phases and phase transitions of rare-gas layers on graphite (001) have been extensively studied.[2] The large surface-to-volume ratios in finely divided graphite (such as exfoliated graphite) allows techniques such as neutron scattering experiments, normally only weakly sensitive to surface phenomena, to be employed. Other studies include thermodynamic measurements of heat capacity,[3] x-ray scattering,[4] low-energy electron diffraction[5] (LEED), and transmission high-energy electron diffraction[6] (THEED). Recently, helium-atom scattering (HAS), which is the most sensitive surface diffraction technique, has been used to study the adsorbate structures.[7]

Inelastic neutron measurements[8] provide only averaged information on the adsorbate phonon dispersion curves since they are only possible using exfoliated graphite, in which the crystallites have random azimuthal orientations. Full dispersion curves have recently been obtained by HAS from Kr and Xe overlayers on Ag(111) and Pt(111) surfaces.[9,10] In comparison to rare-gas-covered metal surfaces, the rare-gas interaction with a graphite surface is characterized by a much larger corrugation in the adsorbate-substrate potential. The surface lattice dynamics of clean single-crystal graphite surfaces have also been recently studied by both HAS (Ref. 11) and electron-energy-loss spectroscopy[12] (EELS).

This paper describes the first HAS measurements of surface phonon dispersion curves for a monolayer of Xe on a graphite surface. Both time of flight (TOF) and angular distributions are obtained. The results are compared with the slab calculations of Rouffignac, Alldredge, and de Wette[13] and important quantitative and qualitative differences are observed.

II. EXPERIMENT

The He-atom spectrometer has been described in detail in Ref. 14. The helium beam is produced in a high-pressure nozzle cooled by a closed-cycle refrigerator, which permits source stagnation temperatures in the range of 55–350 K. At these temperatures the velocity spread $\Delta v/v$ is less than 1%.[15] Most of the measurements were carried out at 18.6 meV incident energy (corresponding to an incident wave vector of $k_i = 5.98$ Å^{-1}) but some runs were also performed at 12.5 meV (4.93 Å^{-1}) and 28.6 meV (7.42 Å^{-1}). The angular spread of the incident beam was collimated to 0.12° full width at half maximum (FWHM), which corresponds to a 1.6-mm-diam spot on the crystal. This small area was imposed by the size of crystallites with uniform orientation on the crystal samples. The sharpest diffraction peaks were found with thin synthetic single crystals[16] with a surface area of about 1×2 mm. Natural crystals[17] invariably showed broadening and splitting of the diffraction peaks, but the smaller diffuse background from the natural crystals indicates an atomically smoother surface. Since the width of the inelastic phonon peaks depends on that of the diffraction peaks all measurements reported in this paper were performed on synthetic crystals. The crystals were cleaved in air and then immediately evacuated. At a target chamber base pressure of 4×10^{-11} Torr the crystal was cleaned at intervals of about 10 h by heating to 700 K for 2 or 3 h.[18]

The scattered He flux is measured with a mass spectrometer at an angle $\theta_{SD} = 90°$ with respect to the incident beam direction. The aperture of the detector is 0.3° FWHM and the overall elastic TOF resolution, determined by the velocity spread of the beam, the chopper pulse, and the length of the ionizer, amounts to about 1.4%.

The xenon monolayers were prepared by exposing the sample to an effusive beam with fluxes in the range of 10^{13}–10^{15} atoms/scm^2. At an initial target temperature of 100 K no xenon adsorption is expected. In order to determine the xenon coverage the intensity of the specularly reflected He beam was monitored while the crystal

was cooled at a rate of 4 K/min. On the onset of condensation, which takes place between 65 and 75 K, depending on the Xe flux, the specular intensity shows a sudden drop by a factor of 10–30. There are three reasons for this loss in specular intensity. (i) The Debye-Waller attenuation is greater since the adsorbate Debye temperature is much lower than the Debye temperature of graphite. (ii) More intensity is scattered into diffraction channels rather than into the specular direction since the xenon surface is much more corrugated than the graphite surface. (iii) The xenon monolayer has additional imperfections and as a result the incoherent scattering is increased at the expense of the specular peak.[19] After condensation of the monolayer the specular intensity begins to rise again with decreasing temperature, mainly because of the reduction in Debye-Waller attenuation. Between 50 and 60 K, depending again on the xenon flux, a second sharp drop in the specular intensity indicates the formation of the bilayer. In all TOF measurements, the xenon flux was kept constant and the temperature of the surface was kept a few degrees above the bilayer formation temperature. Thus, the monolayer is maintained under near equilibrium conditions.

III. RESULTS

Figure 1 shows angular scans of the total scattered He intensity measured along the $\bar{\Gamma}\bar{M}$ (the direction of the carbon-carbon bonds) and the $\bar{\Gamma}\bar{K}$ directions for the clean crystal and for the same crystal covered with a xenon monolayer at three values of the incident wave vector. Whereas the diffraction peaks of the clean surface have a FWHM which is equal to the angular resolution, the superstructure Bragg peaks of the xenon monolayer [in Fig. 1(e)] are noticeably broadened compared to the specular peak. We attribute this to a reduction in coherence length of the xenon covered surface due to the presence of ~ 100 Å domains. In agreement with other work[6] we find that the $\sqrt{3}\times\sqrt{3}R30°$ xenon monolayer is slightly incommensurate with respect to the graphite substrate. The incommensurability has a maximum value of about 6% near the condensation temperature of the monolayer. The adsorbate layer and crystal become commensurate at 1–2 K above the temperature at which condensation of the bilayer occurs. In the diffraction pattern shown in Fig. 1 the observed misfit m, between the Xe lattice and graphite lattice, is given by $(G_{IC}-G_C)/G_C$ and amounts to $1.5\pm 1\%$, where G_{IC} and G_C are the reciprocal-lattice vectors of the incommensurate and commensurate phase, respectively [$G_C(\mathrm{Xe})=1.702$ Å].

Figure 2 shows a series of TOF spectra measured along the $\bar{\Gamma}\bar{K}_R$ and $\bar{\Gamma}\bar{M}_R$ directions, which are the "rotated" boundaries of the irreducible zone of the $\sqrt{3}\times\sqrt{3}R30°$ overlayer (shown in the inset of Fig. 3), at a series of incident angles θ_i between 40° and 44°, corresponding to the left shoulder of the specular maximum of Fig. 1. The largest TOF peak at zero-energy transfer corresponds to elastic scattering of He atoms from surface defects. Slower helium atoms have transferred their energy to phonon modes (phonon creation) and are designated as having negative-energy transfer, while positive-energy

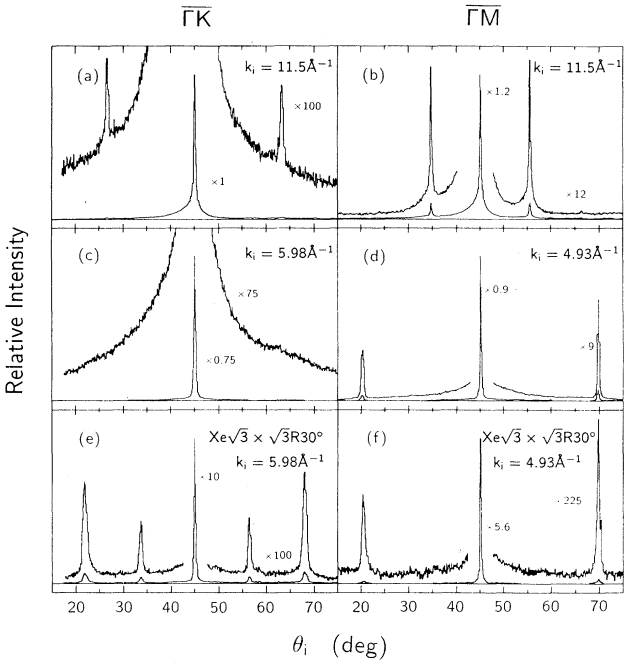

FIG. 1. Angular distributions of helium scattering from the (001) surface of graphite both for the clean and xenon-covered surface. The target temperature is 100 K for the clean graphite, in (e) 60 K, and in (f) 55 K. The intensity of the specular peak in (a) is 2.0 MHz. In all angular distributions a cosine background intensity of 20 kHz at its maximum has been subtracted off. The results indicate that along the $\bar{\Gamma}\bar{K}$ direction graphite is much smoother than along the $\bar{\Gamma}\bar{M}$ direction. A Bragg peak is not observed in (c) because of the low incident wave vector.

transfer refers to helium atoms that have gained energy in the scattering process (phonon annihilation). As can be seen, along both scattering directions there are at least two phonon creation peaks and one annihilation peak. The peak locations indicated by arrows can be assigned with the aid of the "scan curves" plotted at the top of each column in Fig. 2. These scan curves show the kinematic relationship between the energy transfer ΔE and the parallel momentum transfer ΔK for a given set of scattering angles. Dispersion curves are generated from the TOF spectra via these scan curves. Although the spectra are somewhat noisy almost all the spectra show an annihilation phonon peak at +3.2 meV. It is attributed to a nearly flat part of the adlayer dispersion curve with a wave vector larger than 0.4 Å^{-1}. The creation side of the spectra probes the region closer to the origin of the surface Brillouin zone and shows a splitting of the peak with decreasing $+\Delta K$. The splitting is clearly revealed in the sequence of spectra for the $\bar{\Gamma}\bar{M}_R$ direction going from top to bottom. Whereas only one sharp peak is seen at $\theta_i=40°$ a broadened peak is seen at $\theta_i=41°$ which then is split into two peaks spreading apart with increasing angle. The same general trend can be seen in the $\bar{\Gamma}\bar{K}_R$ direction. Note, however, that at $\theta_i=44°$ along $\bar{\Gamma}\bar{K}_R$ the creation peak at -2.8 meV (dashed arrow) is due to the lower mode in the $-\Delta K$ direction as can be seen from the corresponding scan curve. No change in the position of the in-

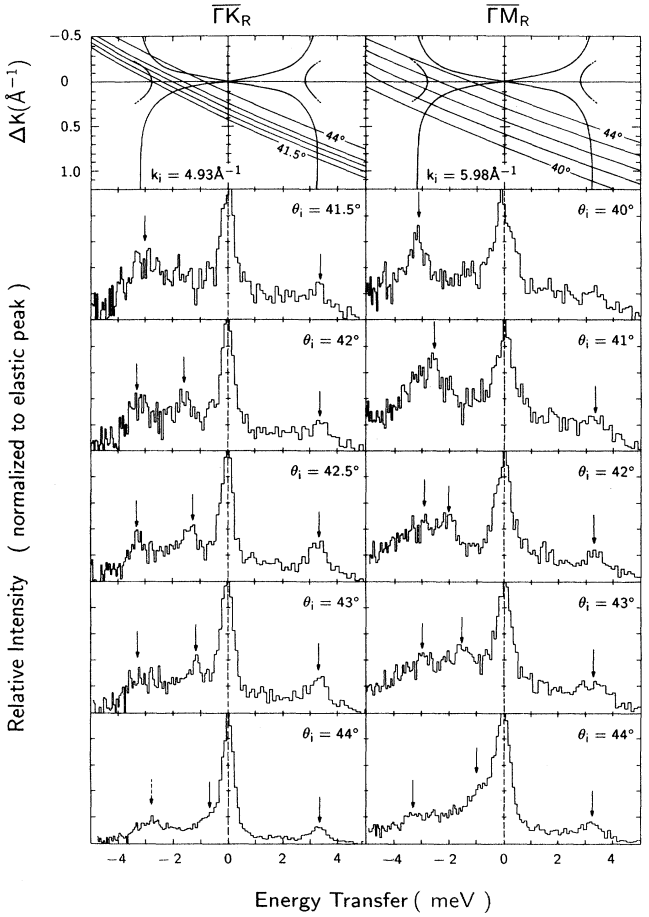

FIG. 2. Helium scattering TOF spectra converted to an energy transfer scale for the xenon-covered graphite along the $\overline{\Gamma K}_R$ and the $\overline{\Gamma M}_R$ direction measured at different incident angles. The incident wave vector is 4.93 Å^{-1} in the $\overline{\Gamma K}_R$ direction and 5.98 Å^{-1} in the $\overline{\Gamma M}_R$ direction. The positions of the phonon peaks indicated by arrows in the TOF spectra are identified in the dispersion curves via the scan curves at the top.

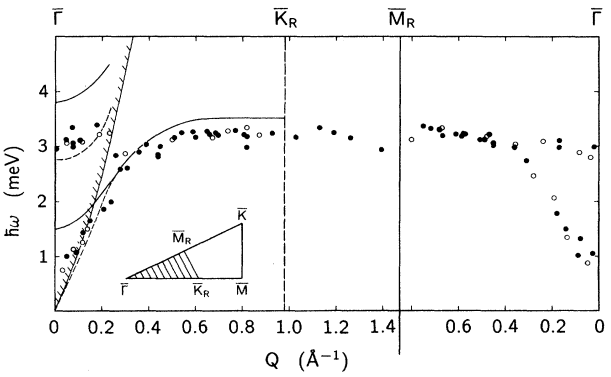

FIG. 3. Experimental phonon dispersion curves for a monolayer of xenon on graphite (001) along the border of the irreducible part of the $\sqrt{3}\times\sqrt{3}R30°$ xenon overlayer Brillouin zone. The solid and dashed lines in the $\overline{\Gamma K}_R$ direction are the results of a slab calculation done by de Rouffignac, Alldrege, and de Wette (Ref. 13). The edge of the transverse bulk band of the clean graphite is indicated by the "shaded" line. The inset displays the irreducible part of the clean graphite ($\overline{\Gamma K M}$) and the $\sqrt{3}\times\sqrt{3}R30°$ xenon overlayer Brillouin zone ($\overline{\Gamma K}_R\overline{M}_R$) ("shaded" area). Open circles identify the data points taken from the TOF spectra of Fig. 2.

elastic TOF peaks could be observed as a function of temperature from $T=55$ to 65 K in these measurements. This suggests that the temperature-dependent incommensurability has no apparent effect on the phonon dispersion curves.

Figure 3 summarizes the data from all the TOF spectra folded onto a dispersion curve along the edges of the irreducible part of the superstructure Brillouin zone. Note that the phonon wave vector $\mathbf{Q}=\mathbf{G}\pm\Delta\mathbf{K}$, where G is the reciprocal-lattice vector of the monolayer. Unfortunately, the available theory is not sufficiently detailed so that one can expect the results to agree with the experimental data. Thus, the only available calculations of de Rouffignac, Alldredge, and de Wette are affected by a coupling of the two surfaces of the slab at wave vectors smaller than about 0.3 Å^{-1}.[13] This is because a relatively thin slab of only 13 layers was used in the calculations. Thus, the pairs of phonon modes with odd and even symmetry with respect to the mirror plane of the slab are split rather strongly and are not degenerate, as they would be for a slab of infinite thickness. Figure 3 also shows the calculated dispersion curves for the sagittal plane vertical (SPV) modes, which have a reasonably large amplitude in the xenon layer. Odd modes are indicated by dashed curves, even modes by solid lines. There are two pairs of such modes. For the upper pair, the amplitude in the xenon layer vanishes at wave vectors larger than 0.2 Å^{-1}. Rouffignac *et al.* suggest that for a slab of infinite thickness there should be only one broad resonance at $\overline{\Gamma}$, centered at about 2.3 meV. Obviously, our data do not agree with this prediction. Instead, we find two maxima near $\overline{\Gamma}$ of which the lower branch coincides very well with the bulk band edge of the pure graphite and tends to $\hbar\omega=0$ at $Q=0$. The other maximum centered at around 3.0 meV must be due to adsorbate-substrate modes. We attribute this mode to a vertically polarized mode. A shear horizontal polarized mode cannot couple to He atoms because of symmetry selection rules and the coupling to a longitudinal would be much weaker and appears not to be observed.

As exemplified by the TOF spectrum at $\theta_i=42°$ ($\overline{\Gamma M}_R$, Fig. 2) and shown in Fig. 3 the data suggest a splitting of about 1 meV in the two modes at about $Q=0.2$ Å^{-1} in both directions. This avoided crossing behavior agrees rather nicely with the model calculations of Hall, Mills, and Black for the lattice dynamics of rare-gas overlayers on smooth surfaces.[20] By modeling the substrate with a continuum model they could avoid the problems at small Q vectors inherent in slab calculations. These predictions have recently been confirmed for Kr on Pt(111).[10] According to this model, there will be an avoided crossing when the adsorbate mode crosses the Rayleigh mode and a broadening of the adsorbate mode frequency distribution which occurs at smaller Q in the transverse bulk band, reflecting the coupling to the bulk modes. This

broadening can be seen in our TOF spectra, but due to the large statistical fluctuations cannot be qualitatively evaluated. As compared to the heavy metal substrates we do, however, expect a much stronger coupling to the substrate modes because of the much smaller mass of the graphite atoms.

ACKNOWLEDGMENTS

We thank H. Suematsu for providing the high-quality synthetic single crystals, G. Brusdeylins and F. W. de Wette for helpful discussions, and K. Madden for critical comments on the manuscript.

[1]R. J. Birgenau and P. M. Horn, Science **232**, 329 (1986).

[2]*Ordering in Two Dimensions,* edited by S. K. Sinha (Elsevier, New York, 1980).

[3]A. Thomy and A. Duval, J. Chem. Phys. **66**, 1966 (1969); **67**, 286 (1970); **67**, 1101 (1970); **74**, 926 (1977).

[4]H. Hong, C. J. Peters, A. Mak, R. J. Birgenau, P. M. Horn, and H. Suematsu, Phys. Rev. B **36**, 7311 (1987).

[5]S. C. Fain, Jr., M. D. Chinn, and R. D. Diehl, Phys. Rev. B **21**, 4170 (1980).

[6]A. Q. D. Faisal, M. Hamichi, G. Raynert, and J. A. Venables, Phys. Rev. B **34**, 7440 (1986).

[7]S. Chung, A. Kara, J. Z. Larese, W. Y. Leung, and D. R. Frankl, Phys. Rev. B **35**, 4870 (1987).

[8]H. Taub, L. Passel, J. K. Kjems, K. Carneiro, J. P. McTague, and J. G. Dash, Phys. Rev. Lett. **34**, 654 (1975).

[9]K. D. Gibson, S. J. Sibener, B. M. Hall, D. L. Mills, and J. E. Black, J. Chem. Phys. **83**, 4256 (1985).

[10]K. Kern, P. Zeppenfeld, R. David, and G. Comsa, Phys. Rev. B **35**, 886 (1987).

[11]G. Benedek, G. Brusdeylins, C. Heimlich, J. P. Toennies, and U. Valbusa, Surf. Sci. **178**, 545 (1986). In recent measurements on another crystal the shear horizontal S_7 mode previously observed could not be reproduced.

[12]J. L. Wilkes, R. E. Palmer, and R. F. Willis, J. Electron Spectrosc. Relat. Phenom. **44**, 355 (1987).

[13]E. de Rouffignac, G. P. Alldredge, and F. W. de Wette, Phys. Rev. B **24**, 6050 (1981).

[14]G. Brusdeylins, R. Doak, and J. P. Toennies, Phys. Rev. B **27**, 3662 (1983).

[15]J. P. Toennies and K. Winkelmann, J. Chem. Phys. **66**, 3965 (1977).

[16]Kish graphite single crystals supplied by H. Suematsu, Institute of Material Science, University of Tsukuba, Sakuramura, Ibaraki 305, Japan.

[17]Ward's Natural Science Establishment, Inc., Rochester, NY.

[18]J. J. Metrois, J. C. Heyrand, and Y. Takeda, Thin Solid Films **51**, 105 (1978).

[19]T. H. Ellis, G. Scoles, U. Valbusa, H. Jonson, and J. H. Weare, Surf. Sci. **155**, 499 (1985).

[20]B. Hall, D. L. Mills, and J. E. Black, Phys. Rev. B **32**, 4932 (1985).